# Characterization and Adsorptive Properties of Pharmaceutical Grade Clays

JEFFREY E. BROWNE *, JOSEPH R. FELDKAMP ‡, JOE L. WHITE ‡, and STANLEY L. HEM *x

Received October 18, 1979, from the *Industrial and Physical Pharmacy Department and the ‡Department of Agronomy, Purdue University, West Lafayette, IN 47907. Accepted for publication January 29, 1980.

**Abstract** □ The adsorption of tetracycline by clays commonly used in pharmacy can be predicted if the identity and character of the commercial clay sample are established. X-ray diffraction, IR spectroscopy, and chemical analysis were used to identify the clay component and any nonclay diluents present in a series of commercial pharmaceutical grade clays. The major clay components were montmorillonite, hectorite, attapulgite, saponite, and kaolinite. The clay structure, the nature of the exchangeable cation, and the presence of nonclay components are important factors affecting the tetracycline–clay interaction. In general, clay structures with a high surface charge lead to a greater interaction with the protonated form of tetracycline, while interaction with the zwitterionic form of tetracycline occurs in clay structures with minimal surface charge. The presence of multivalent, exchangeable cations on the clay surface diminishes interaction with the protonated form of tetracycline. Nonclay components such as calcite and dolomite increase the interactions of the zwitterionic and anionic forms of tetracycline with the clay.

**Keyphrases** □ Tetracycline hydrochloride—adsorption onto clay, interaction with pharmaceutical grade clay, adsorptive properties of clay □ Clay—pharmaceutical grade, adsorption of tetracycline, isomorphous substitution □ Adsorption—tetracycline onto pharmaceutical grade clays

The unique properties of clays have led to their use in pharmaceuticals for both therapeutic effects and excipient action. The crystal structure of clay minerals is well understood, and the behavior of clays in pharmaceutical systems is predictable based on structural considerations. Thus, the identity and characterization of a clay are of prime importance to the pharmaceutical scientist.

The purpose of this study was to illustrate the importance of a complete characterization of clays used in pharmaceuticals so that their behavior in formulations and in a patient's drug regimen can be predicted. The influence of clay structure, the nature of the exchangeable cation, and the presence of nonclay components on the interaction of tetracycline with reference or commercial samples of montmorillonite, hectorite, saponite, attapulgite, and kaolinite were studied.

## BACKGROUND[1]

The basic structure of clays consists of octahedra of aluminum and magnesium in combination with silica tetrahedra to give layer-like or fibrous structures. Cationic-exchange properties can arise in these structures through isomorphous substitution, *i.e.*, aluminum for silicon, magnesium for aluminum, *etc.* A manifestation of isomorphous substitution is the swelling properties of certain clays with high cation-exchange capacity.

The kaolin group of minerals consists of sheets of silica tetrahedra and alumina octahedra shared in a 1:1 ratio. These minerals have little or no isomorphous substitution and normally are nonswelling in aqueous solutions.

Smectites belong to the 2:1 (ratio of silica tetrahedra to alumina and/or magnesia octahedra) structural group of clays and include montmorillonite, hectorite, and saponite. In these structures, an alumina or magnesia octahedral layer is sandwiched between two silica tetrahedral sheets. Structures are designated as dioctahedral when aluminum occupies the octahedral sites and as trioctahedral when magnesium (or other divalent ions) or lithium occupies the octahedral sites.

Isomorphous substitution occurs in both the tetrahedral and octahedral layers of the 2:1 minerals and gives rise to moderate to high cation-exchange capacities.

Isomorphous substitutions also influence the lattice parameters in clays and appear to be correlated to the swelling properties of smectites. As a consequence of the expanding properties, the smectites also possess very high surface areas.

Montmorillonite represents the aluminum-containing smectite group (dioctahedral). The magnesium end member of the smectite group is designated as saponite (trioctahedral). Substitution of lithium for a portion of the magnesium in trioctahedral compositions results in a clay mineral designated as hectorite (trioctahedral).

Fibrous minerals are represented by sepiolite and attapulgite. These minerals are classified as 2:1-type minerals, but the crystal growth is limited to the c dimension, resulting in ribbons of the 2:1 layer attached at their longitudinal edges. A cross section of the fiber gives a checkerboard arrangement of ribbons and voids with no possibility of expansion.

It appears that fibrous minerals have little or no true cation-exchange capacity. However, because of the very thin nature of the ribbons, the external surface area is moderately high. Fibrous minerals also are very porous due to the channels between the ribbons. However, the dimensions of the pores are such that only small molecules such as water, ammonia, and lower alcohols can be accommodated in them.

## EXPERIMENTAL

**Materials**—Tetracycline hydrochloride and all other chemicals were official or reagent grade. Montmorillonite (Wyoming bentonite), hectorite (Hector, Calif.), attapulgite (Georgia palygorskite), and kaolinite (Hydrite-10) were the reference standards[2]. Samples of pharmaceutical grade clays claimed to represent these minerals were obtained commercially as follows: bentonite USP[3], hectorite[4], saponite[5], attapulgite[6], and kaolin NF[7].

Unless otherwise indicated, all clays were used as received.

The sodium form of the reference clays was prepared by washing a 2% suspension of the clay with 1 *M* NaCl. The washing procedure was repeated five times, and excess salt was removed by repeated washing with water until the addition of silver nitrate to the supernate gave a negative chloride test. Clays exhibiting a cation-exchange capacity that were treated in this manner are termed sodium saturated; clays such as kaolinite and attapulgite, which have little or no cation-exchange capacity, are termed sodium treated if washed with sodium chloride in this manner.

The calcium form of montmorillonite was prepared in an analogous manner using 1 *M* $CaCl_2$ as the exchanging solution.

Preliminary examination of the samples of hectorite and commercial saponite by X-ray diffraction showed significant quantities of calcite and dolomite as nonclay diluents. The removal of these carbonates was attempted by a modification of the pH-stat technique (1). A 2% clay sus-

[1] The information in this section is summarized from R. E. Grim, "Clay Mineralogy," 2nd ed., McGraw-Hill, St. Louis, Mo., 1968.

[2] Clay Mineral Repository, Department of Geology, University of Missouri, Columbia, Mo.

[3] R. F. Revson and Co., New York, N.Y.

[4] Macaloid Lot L-917M22B, NL Industries, Industrial Chemicals Division, Hightstown, N.J.

[5] Veegum, R. T. Vanderbilt Co., Norwalk, Conn.

[6] Pharmasorb, Engelhard Minerals and Chemicals Corp., Menlo Park, N.J.

[7] J. T. Baker Chemical Co., Phillipsburg, N.J.



0022-3549/80/0700-0816$01.00/0

pension, 250 ml, was reacted for 24 hr at pH 5.0 in an automatic titration apparatus[8]. The suspension then was washed repeatedly with water until it was salt free as evidenced by the silver nitrate test. The diffractograms of hectorite in Fig. 1 show that the procedure was effective in removing calcite but not dolomite. Clay samples treated in this manner will be referred to as purified.

**X-Ray Diffraction**—Randomly oriented powder specimens of each clay were prepared using the McCreery method (2), and diffractograms[9] were recorded from 5 to 63° 2$\theta$.

The X-ray step scans were used to determine accurately the 060 peak of commercial saponite. A mixture containing 15% silicon[10] was prepared by trituration and filled into a McCreery mount; X-ray step scans were recorded from 58 to 63° 2$\theta$ at a step of 0.02° and a time interval of 90 sec. The 060 spacing of commercial saponite was determined in comparison to the silicon peak at 56.12° 2$\theta$ (3).

The Greene-Kelly test (4) is useful in distinguishing between dioctahedral and trioctahedral structures within the smectite group of clays and was utilized in the characterization of the commercial saponite sample. A 1% clay suspension, consisting of the <2-$\mu$m fraction, was washed five times with 1 *M* lithium chloride. Excess salt then was removed by washing with double-distilled water until it was salt free by the silver nitrate test. The lithium-saturated clay was air dried on a glass slide and then heated to 200–300° for 12 hr. The sample then was saturated with glycerol using the vaporization method (5); X-ray diffractograms were recorded from 3 to 11° 2$\theta$.

Glycerol solvation was used to investigate the presence of montmorillonite-like impurities in attapulgite, commercial attapulgite, kaolinite, and kaolin NF. Glycerol enters montmorillonite-type minerals and causes a characteristic expansion of the basal spacing to ~17.5 Å (6). Glycerol solvation was achieved by dispersing the clay in a 3% glycerol solution through moderate agitation produced by an ultrasonic probe[11]. The dispersions were air dried on a glass slide, and X-ray diffractograms were recorded from 4 to 8° 2$\theta$.

**IR Spectroscopy**—Air-dried films of clay were prepared on zinc sulfide windows[12] (7) and used to record the IR spectra[13].

Studies of pleochroism of the IR bands associated with hydroxyl stretching may be used to determine the orientation of hydroxyl bond axes in layer silicates (8) and were used in characterizing commercial saponite and commercial hectorite. An orientation effect is positive evidence for a structure containing trioctahedral character. Self-supporting clay films were prepared by air drying 1% clay suspensions on polyethylene terephthalate films[14]. The clay films were separated from the polyethylene terephthalate film by bending over a sharp corner. IR spectra of the clay films were recorded from 4000 to 3300 $cm^{-1}$ at perpendicular and various incident angles to the IR beam.

**Transmission Electron Photomicrographs**—Electron microscopic examination[15] of attapulgite was undertaken to confirm the presence of a montmorillonite-type impurity.

**Presence of Organic Matter**—The peroxide test (9) was used to detect organic matter in the clay samples. Thirty milliliters of 30% $H_2O_2$ was added to 15 ml of a 1% clay suspension and heated on a steam plate for 15 min. The treated clay was centrifuged along with an untreated reference suspension. The color of the sample sediment was compared to that of the reference sediment. The presence of organic matter was indicated when the color of the sample sediment was significantly lighter than that of the reference sediment.

**UV Spectroscopic Titrations**—Displacement of the $pK_1$ of tetracycline in clay suspensions was determined by spectroscopic titration. The $pK_{1,eff}$ and partial molar Gibbs free energy, $\Delta\bar{G}_i$, for $H_3T^+$ and $H_2T^\circ$ were calculated from the spectroscopic titration curve using the procedure of Feldkamp and White (10).

Titration curves were constructed by preparing a series of tetracycline–clay suspensions at different $pH^b$ (bulk pH) values and determining the absorbance at 304.1 nm. A typical point on the titration curve was obtained by adding equal volumes of 0.01 *N* HCl or NaOH to two 100-ml volumetric flasks, depending on the $pH^b$ desired. Ten milliliters of a

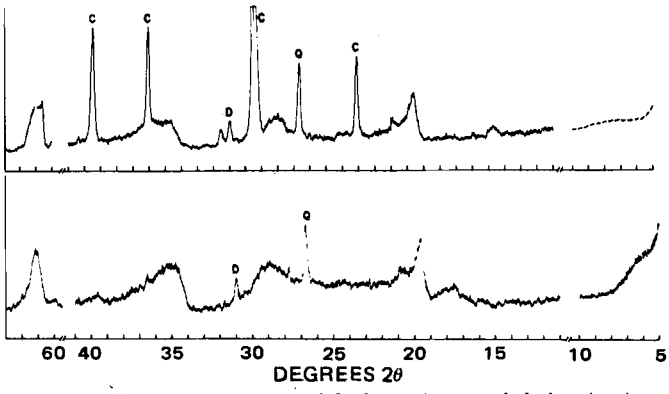


**Figure 1**—*X-ray diffractogram of the hectorite sample before (top) and after (bottom) carbonate removal using the pH-stat technique at pH 5.0. Key: Q, quartz; C, calcite; and D, dolomite. The solid line represents 100 counts/sec (cps) full scale. The dashed line represents 1000 cps full scale.*

200-mg/liter stock solution of tetracycline hydrochloride was added to the sample flask, and the sample and reference flasks were diluted to near volume with double-distilled water. Two milliliters of a 1% clay suspension was added to both flasks, and the flasks were diluted to 100 ml with distilled water. All sample suspensions contained 20 mg of tetracycline and 200 mg of clay/liter. The pH of the sample suspension was determined[16] after the pH reading stabilized. This value was checked by measuring the pH of the supernate ($pH^b$) after centrifugation. These pH readings differed by <1%.

This agreement in pH values was expected since the difference in the pH of the suspension and the pH of the supernate (*i.e.*, the suspension effect) increases as the concentration of the suspension increases (11). The clay suspensions studied were dilute enough so that the pH of the suspension accurately represented the system, *i.e.*, $pH_{susp} \simeq pH^b$.

The difference in the absorbance of the sample and the reference suspension ($A_s - A_r$) was measured and plotted *versus* $pH^b$ to construct the titration curves.

**Adsorption**—The fraction of tetracycline bound by the clay at different $pH^b$ conditions was determined using the samples from the spectroscopic titration experiment. A sample of each suspension was centrifuged, and 15 ml of supernate was collected. Sufficient hydrochloric acid was added to ensure that all of the tetracycline was in the protonated form. The absorbance was measured at 304.1 nm.

The fraction bound, $f$, was calculated from:

$$f = \frac{A_0 - (A_s - A_r)}{A_0} \qquad \text{(Eq. 1)}$$

where $A_0$ is the absorbance of a tetracycline solution (20 mg/liter) containing only the protonated form of tetracycline.

## RESULTS AND DISCUSSION

**Montmorillonite**—The X-ray diffractogram of bentonite USP is compared to sodium-saturated montmorillonite in Fig. 2. A comparison of the reflections indicates that montmorillonite was the major clay component in bentonite USP. However, peaks other than those established for montmorillonite appeared in the region between 11 and 41° 2$\theta$ in the bentonite USP sample. The intense peak at 26.64° 2$\theta$, corresponding to an interplanar spacing of 3.55 Å, indicates the presence of quartz (12). Other less intense peaks occurring at 11.7, 20.76, and 29.18° 2$\theta$, corresponding to spacings of 7.56, 4.27, and 3.059 Å, are typical of gypsum (12). The peaks at 23.10, 29.42, and 39.40° 2$\theta$, corresponding to spacings of 3.85, 3.035, and 2.285 Å, are associated with calcite (12).

The IR spectra shown in Fig. 3 also indicate that montmorillonite was the major clay constituent in the bentonite USP sample. Characteristic absorption bands for montmorillonite were observed in both samples at 3620, 1200–1000, 915, 878, and 850 $cm^{-1}$ (13–15).

The presence of organic material was confirmed in bentonite USP but not in sodium-saturated montmorillonite using the peroxide test.

The dominant exchangeable cation in the bentonite USP sample was sodium, although 7.1 and 2.7% of the exchange capacity were satisfied by calcium and magnesium ions, respectively (7).

[8] PHM 26 pH meter, TTT II titrator, ABU12 autoburet, TTA3 titration assembly, and SBR2 recorder, Radiometer, Copenhagen, Denmark.

[9] Siemens A G Kristalloflex 4 generator and type F diffractometer, Karlsruhe, West Germany.

[10] Silcon powder, 100 mesh, Alfa Inorganics, Beverly, Mass.

[11] Model W185 sonifier cell disruptor, Heat Systems-Ultrasonic, Plainview, N.Y.

[12] Irtran 2, Eastman Kodak Co., Rochester, N.Y.

[13] Model 180, Perkin-Elmer Corp., Norwalk, Conn.

[14] Mylar.

[15] Hitachi HU-11 100-kv electron microscope, Hitachi Ltd., Tokyo, Japan.

[16] Model 801, Orion Research, Cambridge, Mass.

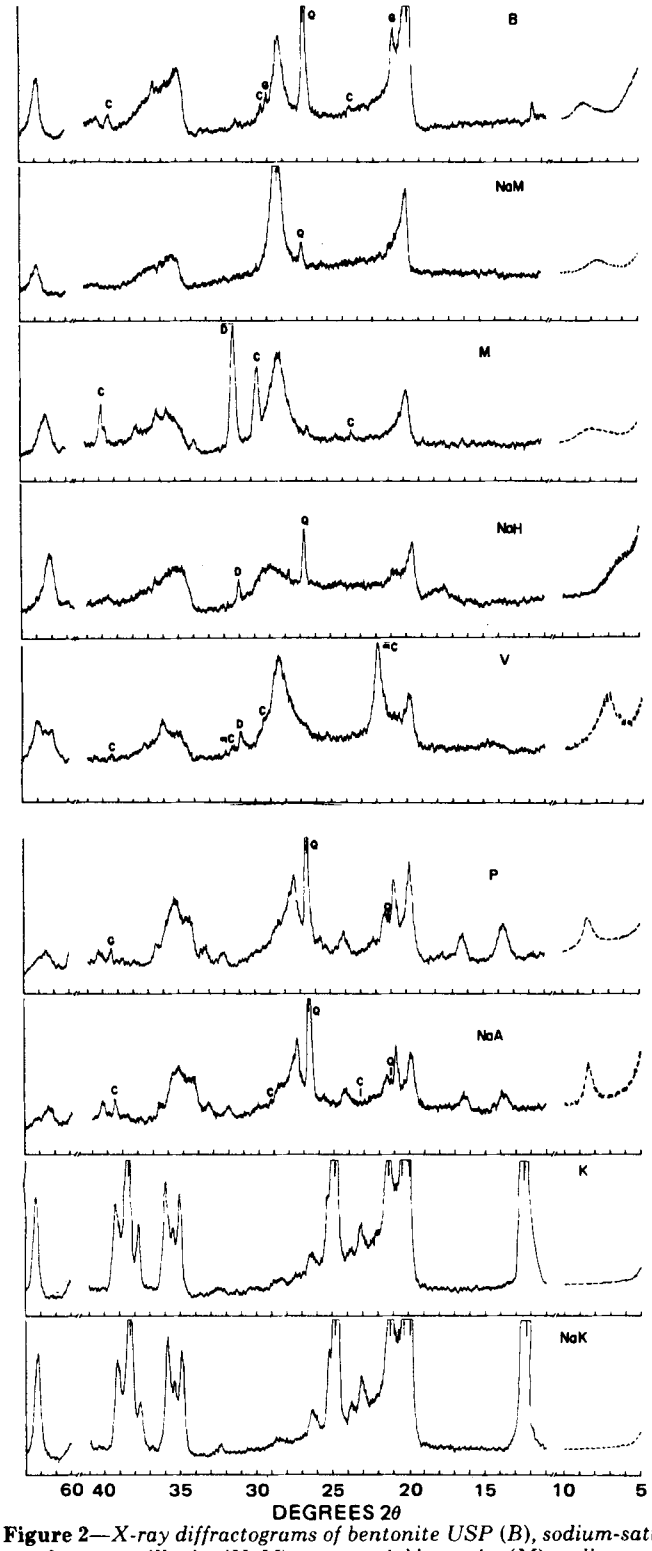


**Figure 2**—*X-ray diffractograms of bentonite USP (B), sodium-saturated montmorillonite (NaM), commercial hectorite (M), sodium-saturated hectorite (NaH), commercial saponite (V), commercial attapulgite (P), sodium-treated attapulgite (NaA), kaolin NF (K), and sodium-treated kaolinite (NaK). Peaks corresponding to quartz (Q), gypsum (G), dolomite (D), calcite (C), and α-cristobalite (αC) are identified. The solid line represents 100 cps full scale. The dashed line represent 1000 cps full scale.*

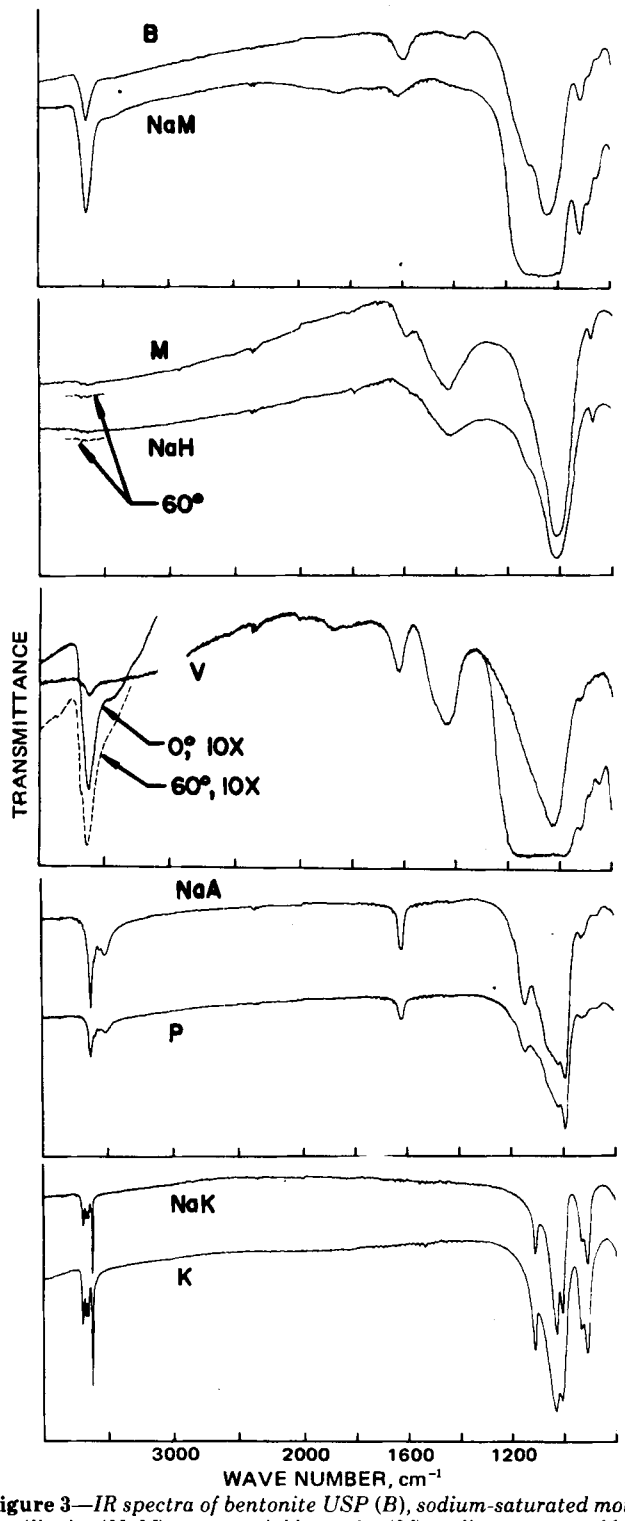


**Figure 3**—*IR spectra of bentonite USP (B), sodium-saturated montmorillonite (NaM), commercial hectorite (M), sodium-saturated hectorite (NaH), commercial saponite (V), commercial attapulgite (P), sodium-treated attapulgite (NaA), kaolin NF (K), and sodium-treated kaolinite (NaK).*

These findings for the composition of the bentonite USP sample are consistent with previous reports, which indicated that sodium montmorillonite is the major component of bentonite USP (16, 17). However, exchangeable calcium and magnesium ions may constitute 35–65% of the exchange capacity of bentonite USP, and bentonite USP has been found to contain 10–15% quartz as the primary nonclay diluent (18). Other nonclay minerals known to affect the behavior of bentonites include gypsum, calcite, biotite, feldspar, and cristobalite.

The effect of the exchangeable cation on the adsorptive properties of bentonite USP will be illustrated by examining the interaction of bentonite USP, sodium-saturated montmorillonite, and calcium-saturated montmorillonite with tetracycline. As indicated in Table I, interaction with all three forms of montmorillonite caused a shift in the first acid–base equilibrium of tetracycline so that the apparent equilibrium constant

**Table I—Effects of Pharmaceutical Grade Clays on the First Acid–Base Equilibrium of Tetracycline**

| Clay | $pK_{1,eff}$ | $\Delta\bar{G}_{H_3T^+}$, kcal/mole | $\Delta\bar{G}_{H_2T^0}$, kcal/mole |
|---|---|---|---|
| Control | 3.34 | — | — |
| Bentonite USP | 4.15–4.74 | −1.13–−1.93 | −0.11–−0.16 |
| Sodium-saturated montmorillonite | 6.23 | −3.99 | −0.03 |
| Calcium-saturated montmorillonite | 4.39 | −1.92 | −0.47 |
| Purified, sodium-saturated hectorite | 5.99 | −3.52 | −0.04 |
| Commercial saponite | 4.27 | −1.26 | −0.17 |
| Purified, sodium-saturated commercial saponite | 5.23 | −2.97 | −0.05 |
| Commercial attapulgite | 3.51 | −0.33 | −0.14 |
| Sodium-treated attapulgite | 3.46 | −0.20 | −0.07 |
| Sodium-treated kaolinite | 3.02 | 0.00 | −0.16 |

($pK_{1,eff}$) was significantly different than that observed in solution ($pK_1$). The magnitude of the shift reflects the degree of perturbation of the equilibrium (10). The greatest shift resulted from interaction with sodium-saturated montmorillonite.

The $pK_{1,eff}$ values of tetracycline in the presence of the sodium and calcium forms of montmorillonite, 6.23 and 4.39, respectively, remained relatively constant over the $pH^b$ range of interest, indicating that $pK_{1,eff}$ was independent of $pH^b$. However, the $pK_{1,eff}$ values ranged from 4.15 to 4.74, depending on the $pH^b$ of the bentonite USP suspension. This dependency of $pK_{eff}$ on $pH^b$ is attributed to the presence of organic material in the bentonite USP sample since $pK_{eff}$ was found to be dependent on $pH^b$ in suspensions of organic-containing soils (19).

The relative strength of the interaction of the clay with the protonated, $H_3T^+$, or zwitterionic, $H_2T^0$, form of tetracycline is expressed by the magnitude of $\Delta\bar{G}_i$ given in Table I, where $\Delta\bar{G}_i$ is the change in the partial molar Gibbs free energy accompanying the addition of clay to the system. Sodium-saturated montmorillonite interacted strongly with $H_3T^+$ but showed virtually no interaction with $H_2T^0$. In contrast, calcium-saturated montmorillonite and bentonite USP showed less interaction with $H_3T^+$, but the $\Delta\bar{G}_{H_2T^0}$ value indicates that a weak interaction occurred with the zwitterionic form.

The fraction of tetracycline bound to the clay (Fig. 4) also indicates that sodium-saturated montmorillonite only interacted with the cationic form because adsorption was observed only under $pH^b$ conditions when $H_3T^+$ was present.

Tetracycline was bound strongly by calcium-saturated montmorillonite (Fig. 4) under pH conditions favoring the cationic form, as evidenced by the maximum at pH 2.7. However, adsorption also occurred at $pH^b$ conditions favoring the zwitterionic and anionic forms, which caused the secondary maximum at pH 8.

Increased adsorption of tetracycline by calcium-saturated montmorillonite above pH 9.5 is due to complexation of the $T^{2-}$ form of tetracycline with exchangeable calcium ions to form a positively charged calcium–tetracycline complex, which is adsorbed readily by the negative clay surface. The added sodium ions (arising from the sodium hydroxide needed to adjust the pH) cause the displacement of calcium ions from the clay. These calcium ions are available to form higher calcium–tetracycline complexes, which are positively charged and therefore are adsorbed by the clay.

The fraction bound curve for the bentonite USP sample (Fig. 4) showed a maximum adsorption of ~80% of the tetracycline in the system. This degree of adsorption was significantly less than the maximum adsorption of tetracycline by sodium- or calcium-saturated montmorillonite.

The adsorption of tetracycline by bentonite USP had a greater similarity to the fraction bound curve of calcium-saturated montmorillonite than to the fraction bound curve of sodium-saturated montmorillonite. The presence of calcium and magnesium as exchangeable cations in the bentonite USP sample and the calcite impurity was responsible for adsorption of tetracycline at pH conditions where no adsorption would be expected if the montmorillonite were completely sodium saturated.

The lower maximum adsorption of tetracycline by bentonite USP in comparison to sodium-saturated montmorillonite probably was due to the significant nonclay component, which includes quartz, gypsum, calcite, and organic material.

Thus, the nature of the exchangeable cations and the amount of nonclay material have a significant effect on tetracycline adsorption by bentonite USP.

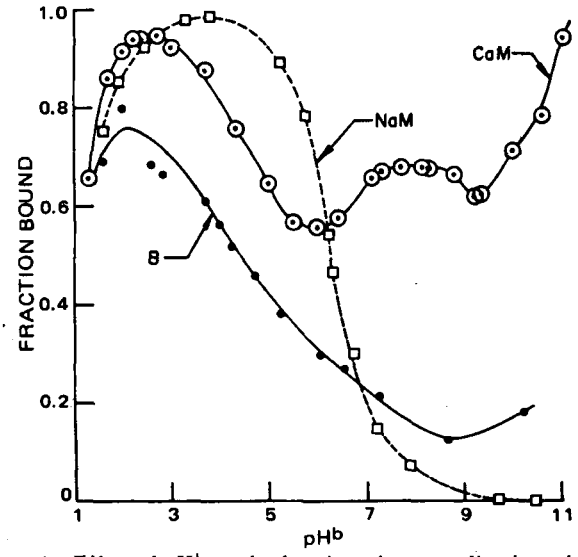


**Figure 4**—*Effect of $pH^b$ on the fraction of tetracycline bound* (f) *in sodium-saturated montmorillonite (NaM), calcium-saturated montmorillonite (CaM), and bentonite USP (B) suspensions.*

**Hectorite**—In general, the X-ray reflections for commercial hectorite in Fig. 2 correspond fairly well to those for purified, sodium-saturated hectorite, indicating that hectorite was the major clay mineral contained in the commercial hectorite sample. However, in the region between 60 and 63° 2$\theta$, the 060 reflection of the samples of commercial hectorite and purified, sodium-saturated hectorite had unequal spacings of 1.509 and 1.514 Å, respectively. These differences were expected and probably reflect composition differences due to the amount of lithium substituted for magnesium within the clay structure.

Several nonclay peaks were observed for the sample of commercial hectorite in the region from 11 to 41° 2$\theta$. A very strong, sharp peak was located at 31.12° 2$\theta$, corresponding to a spacing of 2.87 Å, a characteristic spacing for dolomite (11). Additional peaks were found at the established spacings for calcite (3.85, 3.035, and 2.285 Å) and quartz (3.35 Å).

The IR spectra of commercial hectorite and purified, sodium-saturated hectorite (Fig. 3) were essentially identical, thus confirming that hectorite was the major clay contained in the commercial hectorite sample. The absorption shoulder at 1012 $cm^{-1}$ and a weak absorption shoulder at 1120 $cm^{-1}$ typically are observed in hectorite samples. Large quantities of carbonate minerals (calcite and dolomite) were indicated by the 1430- and 877-$cm^{-1}$ bands.

Pleochroism can be used to identify dioctahedral and trioctahedral structures in the smectite group. In trioctahedral minerals, such as hectorite, the transition moment of the hydroxyl group is perpendicular to the plane of the layer, while the hydroxyl groups are tilted out of the plane in dioctahedral minerals (8). Thus, the orientation of an oriented film of a trioctahedral mineral will affect the intensity of the hydroxyl absorbance bands but the IR spectra of dioctahedral minerals are not affected.

Oriented films of commercial hectorite and hectorite, both trioctahedral, are expected to show an orientation effect. When perpendicular to the IR beam, the absorption band at 3680 $cm^{-1}$, corresponding to the stretching frequency of structural hydroxyl groups in a magnesium-containing trioctahedral mineral, was absent in both spectra (Fig. 3). No increase in intensity was observed at 3680 $cm^{-1}$ when the oriented films were placed at 60° incidence to the IR beam. This finding suggests that the structural hydroxyl groups were replaced by fluorine atoms. These findings agree well with a chemical analysis of hectorite, which indicated the presence of 4.5% fluorine (20).

It was not possible to examine the acid–base equilibria of tetracycline in the presence of commercial hectorite due to severe light scattering. To obtain some indication of the interaction of commercial hectorite with tetracycline, the behavior of tetracycline in the presence of purified, sodium-saturated hectorite was studied. Annoying light-scattering effects did not occur for titrations performed in purified, sodium-saturated hectorite suspensions. Thus, both the presence of carbonate impurities and multivalent ions as exchangeable cations appear to affect significantly the dispersion state of the clay.

As seen in Table I, the displacement of the first acid–base equilibrium of tetracycline in the presence of purified, sodium-saturated hectorite

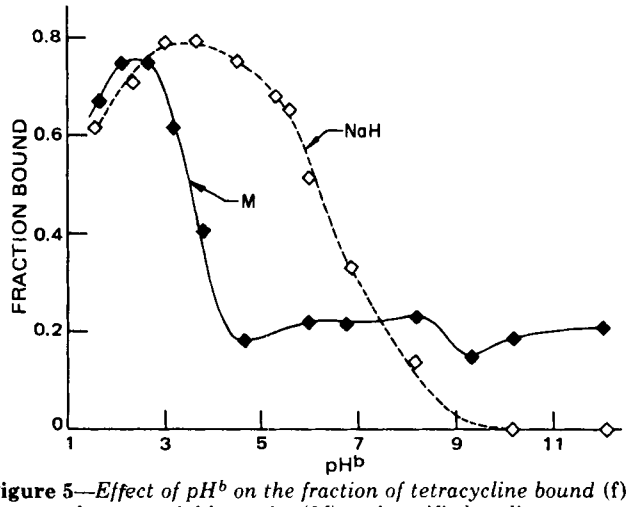


**Figure 5**—*Effect of $pH^b$ on the fraction of tetracycline bound (f) in untreated commercial hectorite (M) and purified, sodium-saturated hectorite (NaH) suspensions.*

was almost as large as that produced by sodium-saturated montomorillonite. The $pK_{1,eff}$ value of 5.99 remained fairly constant over the $pH^b$ range, indicating that $pK_{1,eff}$ was independent of $pH^b$. The $H_3T^+$ species was strongly stabilized by purified, sodium-saturated hectorite, as indicated by the large value of $\Delta\overline{G}_{H_3T^+}$, although virtually no interaction with $H_2T^0$ was observed.

The fraction bound curve for purified, sodium-saturated hectorite (Fig. 5) showed that adsorption of tetracycline occurred under $pH^b$ conditions where $H_3T^+$ was present. This adsorption pattern was expected based on the structural similarities between hectorite and montmorillonite. However, a lower maximum was observed in the presence of purified, sodium-saturated hectorite in comparison to sodium-saturated montmorillonite (Fig. 4). It is believed that protons more effectively compete with $H_3T^+$ for the negative charge sites on the surface of hectorite than on montmorillonite due to differences in the distribution of negative charges arising from the clay structure.

In contrast, the fraction bound curve for commercial hectorite showed a constant adsorption above $pH^b$ 4 in addition to a maximum at $pH^b$ 2.7. The adsorption maximum is believed to represent adsorption of $H_3T^+$ by the hectorite present in the sample of commercial hectorite, while the constant adsorption above $pH^b$ 4 may be due to complexation of the zwitterionic and anionic species of tetracycline with calcium in the nonclay components. Stern (21) reported that the anionic species of tetracycline is adsorbed onto calcium fluoride surfaces. In a similar manner, it is proposed that tetracycline is adsorbed onto the surfaces of calcite and dolomite present in commercial hectorite.

The adsorptive properties of commercial hectorite cannot be understood based on the structure of hectorite. However, the adsorptive properties of commercial hectorite are predictable when the nonclay components are recognized.

**Saponite**—The X-ray analysis of commercial saponite (Fig. 2) showed reflections typical of the smectite group of clay minerals. In addition to the smectite reflections, a very sharp, strong peak was noted at 21.40° $2\theta$, corresponding to an interplanar spacing of 4.15 Å. This peak and a much less intense peak at 31.38° $2\theta$ (2.845 Å) indicated the presence of $\alpha$-cristobalite (12) in the commercial saponite sample. Other peaks in the region from 11 to 41° $2\theta$ corresponded to dolomite and calcite.

As seen in Fig. 6, the X-ray step scan of the 060 reflection of the commercial saponite sample resulted in spacings at 62.02 and 61.01° $2\theta$, corresponding to spacings of 1.496 and 1.518 Å. The dioctahedral smectite minerals, such as montmorillonite, have a characteristic 060 spacing of 1.48–1.50 Å, while the trioctahedral smectites, such as saponite and hectorite, are characterized by a spacing of 1.51–1.53 Å for the 060 reflection (22). The 060 reflections suggest that commercial saponite is a mixture of dioctahedral and trioctahedral smectites, with the sample being richer in the dioctahedral component based on the larger peak at 1.496 Å.

The IR spectrum (Fig. 3) of oriented films of the commercial saponite sample produced a number of absorbance bands whose assignments are characteristic of montmorillonite. The absorption band at 3620 $cm^{-1}$ was similar to the hydroxyl-stretching frequency observed in montmorillonite. Characteristic bands for hydroxyl-bending frequencies in montmorillonite at 915, 878, and 850 $cm^{-1}$ also were found in the spectra for commercial saponite. Carbonates are indicated due to the large absorption band at 1430 $cm^{-1}$.

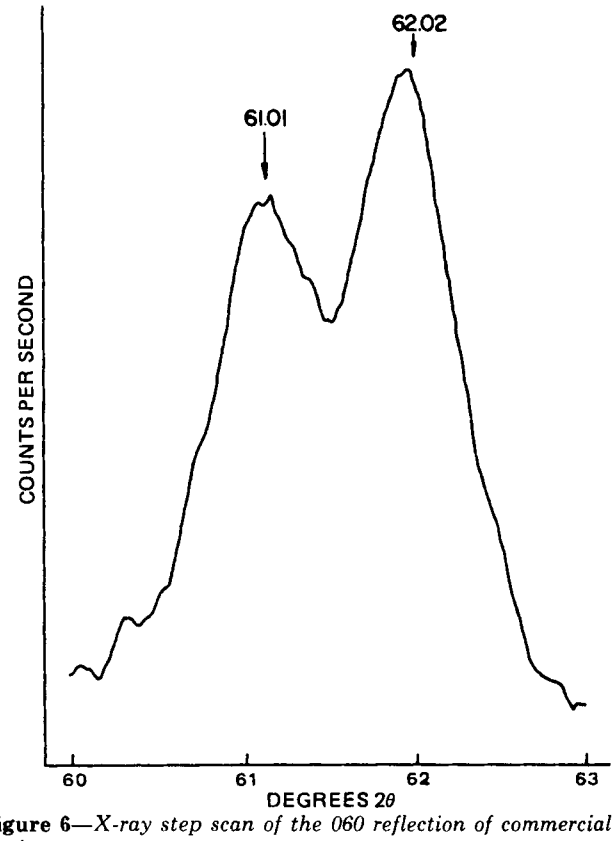


**Figure 6**—*X-ray step scan of the 060 reflection of commercial saponite.*

An orientation effect was observed in the 10× magnification of the IR spectrum of commercial saponite (Fig. 3) when the sample was placed at 60° incidence to the beam. This prompted further pleochroic studies of commercial saponite, which established the presence of dioctahedral and trioctahedral structures in the clay.

As seen in Fig. 7, the intensity of the band at 3680 $cm^{-1}$ increased with the angle of rotation, confirming the presence of a trioctahedral smectite in commercial saponite. A dioctahedral mineral also was present since no orientation effect was observed for the IR band at 3620 $cm^{-1}$, which was assigned to the characteristic hydroxyl-stretching frequency of dioctahedral structures. Thus, IR analysis also indicated that the commercial saponite was a mixture of dioctahedral and trioctahedral mineral phases.

Figure 8 shows the results of the Greene-Kelly test on commercial saponite. This test depends on the observation that lithium-saturated smectites (dioctahedral) collapse irreversibly when heated to 200–300°, whereas the collapse of trioctahedral smectites treated similarly is reversible. Upon glycerol solvation of commercial saponite, a collapsed basal (001) spacing of 9.5 Å and an expanded 001 spacing of 18.4 Å were observed, which indicated the presence of dioctahedral and trioctahedral components.

Both X-ray and IR analyses indicated that the commercial saponite sample contained a mixture of dioctahedral and trioctahedral minerals and several nonclay components. The conclusion was supported by a chemical analysis, which reported 13.7% equivalent magnesium oxide in the commercial saponite sample (23). Ross and Hendricks (24) reported the equivalent magnesium oxide content of several montmorillonite samples and found a range of 0.16–8.67% equivalent magnesium oxide. Their analysis of a group of trioctahedral smectites, including saponites and hectorites, yielded an equivalent magnesium oxide content, which ranged from 19.4 to 26.5%.

Because no known smectite mineral contains 13.7% equivalent magnesium oxide and the X-ray and IR studies clearly showed both dioctahedral and trioctahedral character, it is concluded that the sample of commercial saponite was not a one-phase material but a mixture of at least two phases, one similar to montmorillonite and a lesser phase similar to saponite.

The commercial saponite sample caused a shift of the first acid–base

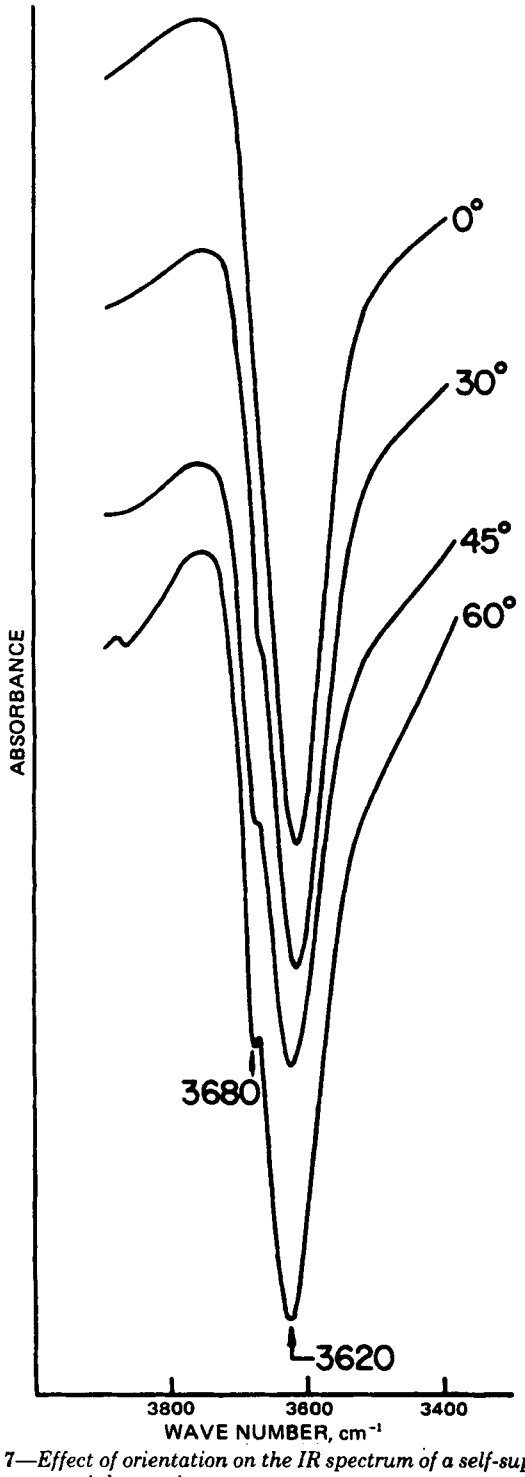


**Figure 7**—*Effect of orientation on the IR spectrum of a self-supporting film of commercial saponite.*

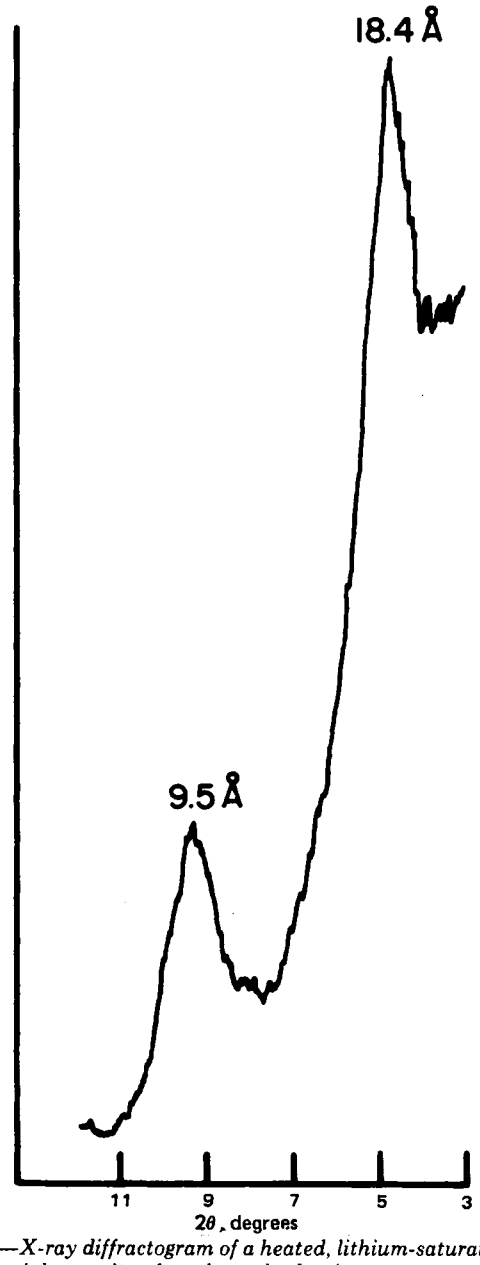


**Figure 8**—*X-ray diffractogram of a heated, lithium-saturated sample of commercial saponite after glycerol solvation.*

equilibrium of tetracycline to a $pK_{1,eff}$ of 4.27 (Table I). This shift reflects a much stronger interaction with $H_3T^+$ than $H_2T^0$, as indicated by the $\Delta\bar{G}_i$ values reported in Table I.

Because both montmorillonite and saponite contain exchangeable cations and the commercial saponite sample contains nonclay diluents, the effect of commercial saponite on the acid–base equilibrium of tetracycline also was studied following purification to remove carbonate impurities and sodium saturation. The displacement in the acid–base equilibrium of tetracycline was much greater in the presence of the purified, sodium-saturated commercial saponite than that observed for commercial saponite (Table I).

The findings are similar to the values observed with sodium-saturated montmorillonite and purified sodium-saturated hectorite, the other smectite minerals studied. Thus, it appears that exchangeable cations other than sodium are present in commercial saponite.

The fraction bound curve for tetracycline in the presence of purified, sodium-saturated commercial saponite (Fig. 9) was very similar to the adsorption profile seen for sodium-saturated montmorillonite (Fig. 4) and purified, sodium-saturated hectorite (Fig. 5). Adsorption only occurred when $pH^b$ conditions permitted $H_3T^+$ to be present and was close to 100% at the $pH^b$ of maximum adsorption.

The fraction bound curve for tetracycline in a commercial saponite suspension showed a lower maximum fraction bound and also indicated that adsorption occurred at higher $pH^b$ conditions, where the zwitterionic and anionic forms of tetracycline were present. As with bentonite USP and commercial hectorite, the unexpected adsorption profile for commercial saponite is attributed to the effects of the exchangeable cations and the nonclay impurities present in the sample.

**Attapulgite**—Examination of the X-ray diffractograms in Fig. 2 for commercial attapulgite and sodium-treated attapulgite indicates that attapulgite is the major clay component of commercial attapulgite. Peaks corresponding to quartz and calcite also were seen in the diffractograms. In addition, the presence of a montmorillonite-like component in both commercial attapulgite and sodium-treated attapulgite is suggested since treatment of each sample with glycerol resulted in an expanded spacing

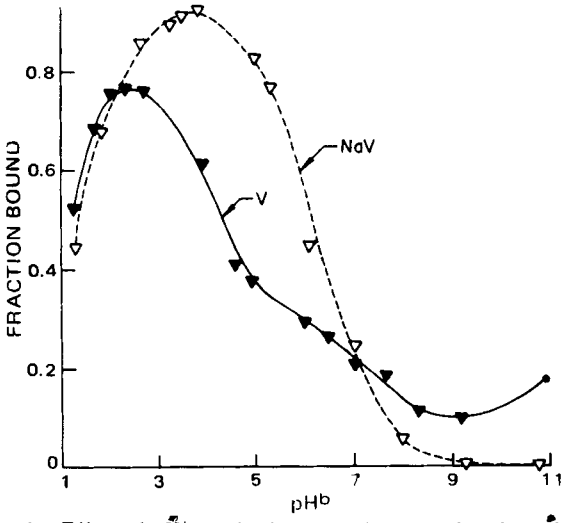


**Figure 9**—*Effect of $pH^b$ on the fraction of tetracycline bound (f) in untreated commercial saponite (V) and purified, sodium-saturated commercial saponite (NaV) suspensions.*

of 14.5 and 15.2 Å for the 001 reflection of commercial attapulgite and sodium-treated attapulgite, respectively.

Cation-exchange capacity values have been reported for attapulgite. However, some of the higher values reported were attributed to montmorillonite impurities (25).

Transmission electron photomicrographs of sodium-treated attapulgite (Fig. 10) showed elongated, lath-shaped particles characteristic of attapulgite. The irregularly shaped aggregates interwoven among the attapulgite fibers are believed to be the montmorillonite-like impurity and illustrate the difficulty of obtaining pure attapulgite samples.

The IR spectra (Fig. 3) of commercial attapulgite and sodium-treated attapulgite were essentially identical. Both spectra showed the characteristic IR bands for attapulgite at 3625, 3595, 3560, 3505, 1192, 1145, 1090, 1036, 988, and 925 $cm^{-1}$. Very weak bands were noted at 1425 and 876 $cm^{-1}$, corresponding to calcite.

A shift of only 0.17 pK unit was observed in the first acid–base equilibrium of tetracycline in the presence of commercial attapulgite (Table I) and was accompanied by a small change in the partial molar Gibbs free energy of the $H_3T^+$ species. No substantial interaction was expected based on the cation-exchange capacity arising from the clay's structure. The observed interaction is believed to be due largely to interaction of $H_3T^+$ with the montmorillonite-type impurity in commercial attapulgite.

The effect of $pH^b$ on the fraction of tetracycline bound to the sample of commercial attapulgite also indicates the presence of a montmorillonite-like component. A maximum in the fraction bound curve (Fig. 11) was observed at $pH^b$ conditions favoring the protonated species, $H_3T^+$. This maximum arose from the cation-exchange capacity due to any isomorphous substitution in attapulgite and the contribution of the montmorillonite. The degree of adsorption decreased from the maximum of 35% as the $pH^b$ increased. Adsorption remained relatively constant at ~15% at pH conditions that favor the zwitterionic and anionic forms of tetracycline.

Although calcium from the calcite impurity may reduce the amount of tetracycline in solution through the formation of calcium–tetracycline complexes, it is more likely that the constant, weak adsorption observed above $pH^b$ 5 was due to physical adsorption. This type of adsorption pattern is expected based on the uncharged structure of attapulgite.

The selective adsorption of the $H_3T^+$ species indicated by the maximum at $pH^b$ 3 is the adsorption pattern typical of the montmorillonite group of clays and indicates the important effect of the montmorillonite-like impurity on the adsorptive properties of commercial attapulgite.

Sodium-treated attapulgite caused a slightly smaller displacement of the first acid–base equilibrium of tetracycline than did commercial attapulgite and thus resulted in a smaller effect on $pK_{1,eff}$ (Table I). It was less effective in adsorbing tetracycline in comparison to commercial attapulgite (Fig. 11). It is believed that the heat and acid treatments employed to activate commercial attapulgite increase the availability of adsorption sites in attapulgite due to either an increase in the specific surface area of commercial attapulgite or the removal of adsorbed species. Thus, the fraction of tetracycline bound by commercial attapulgite was greater throughout the entire pH range than was observed for sodium-treated attapulgite.

**Kaolinite**—Identical X-ray diffractograms (Fig. 2) were obtained for sodium-treated kaolinite and kaolin NF and were characteristic of


**Figure 10**—*Electron photomicrograph of sodium-treated attapulgite showing the elongate lath-shaped particles (A) that are characteristic of attapulgite and the irregularly shaped aggregates (M) believed to be the montmorillonite-like impurity (magnification = 30,000×).*

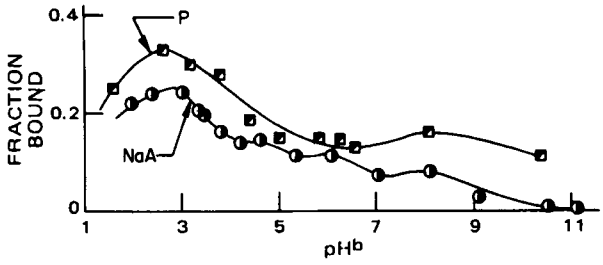


**Figure 11**—*Effect of $pH^b$ on the fraction of tetracycline bound* (f) *in commercial attapulgite (P) and sodium-treated attapulgite (NaA) suspensions.*

kaolinite, indicating that kaolinite is the major clay present in kaolin NF. Both samples were pure as evidenced by the absence of reflections corresponding to nonclay diluents and the absence of expansion following glycerol treatment.

The IR absorption spectra of sodium-treated kaolinite and kaolin NF showed the characteristic IR bands for kaolinite at 3695, 3670, 3650, 3620, 1108, 1038, 1012, 940, and 915 $cm^{-1}$ (Fig. 3).

Light scattering prevented the study of the acid–base equilibrium of tetracycline in the presence of kaolin NF. However, the first acid–base equilibrium of tetracycline in the presence of sodium-treated kaolinite was examined. As seen in Table I, $pK_{1,eff}$ was decreased slightly in the presence of sodium-treated kaolinite, indicating a displacement in favor of the zwitterionic form of tetracycline. No interaction was found with $H_3T^+$, but a weak interaction was observed with $H_2T^0$, as evidenced by the $\Delta\bar{G}_{H_2T^0}$ value of −0.2 kcal/mole.

This behavior is in contrast to the effect of montmorillonite, hectorite, and commercial saponite, where $pK_{1,eff}$ increased due to stabilization of $H_3T^+$ by the clay. However, kaolinite has little or no cation-exchange capacity and hence no stabilization of $H_3T^+$ occurs. The shift of $pK_{1,eff}$ in favor of $H_2T^0$ is consistent with the structure of kaolinite.

Since kaolinite is a nonexpanding mineral, the edge surface comprises a substantial portion (10–20%) of the total surface area. Broken bonds at the edges of the tetrahedral sheet give rise to a small permanent positive charge. A negative charge whose magnitude is related directly to pH results from broken edges of the octahedral sheet (26). Thus, at low $pH^b$ conditions, kaolinite exhibits a small positive charge arising from the tetrahedral sheet; at higher $pH^b$ conditions, the negative charge from the octahedral sheet predominates.

The fraction bound curve for tetracycline in the presence of sodium-treated kaolinite (Fig. 12) showed a very low degree of adsorption. The adsorption profile can be related to the pH-dependent charge arising from broken edges. No adsorption is seen at low $pH^b$ values because the $H_3T^+$ species is repelled by the positive edge charge. Likewise, at basic $pH^b$ conditions, the anionic forms of tetracycline are repelled by the negative edge charge. A small degree of physical adsorption occurs in the $pH^b$ range where the $H_2T^0$ species is present.

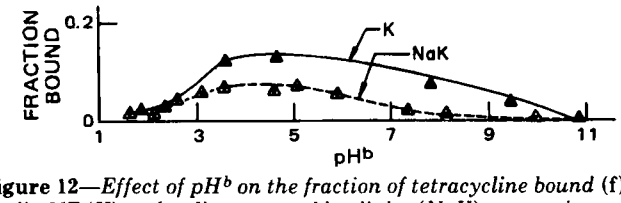


**Figure 12**—*Effect of $pH^b$ on the fraction of tetracycline bound* (f) *in kaolin NF (K) and sodium-treated kaolinite (NaK) suspensions.*

The fraction bound curve (Fig. 12) for tetracycline in the presence of kaolin NF showed a similar adsorption profile to that of sodium-treated kaolinite. This finding was expected because both X-ray and IR analyses showed that kaolin NF was pure kaolinite.

## REFERENCES

(1) N. J. Kerkhof, J. L. White, and S. L. Hem, *J. Pharm. Sci.*, **66**, 1528 (1977).

(2) H. P. Klug and L. E. Alexander, "X-ray Diffraction Procedures for Polycrystalline and Amorphous Materials," Wiley, New York, N.Y., 1954, p. 300.

(3) W. Parrish, *Acta Crystallogr.*, **13**, 838 (1960).

(4) R. Greene-Kelly, *J. Soil Sci.*, **4**, 233 (1953).

(5) G. Brunton, *Am. Mineral.*, **40**, 124 (1955).

(6) D. M. C. MacEwan, *Nature (London)*, **154**, 577 (1944).

(7) L. S. Porubcan, C. J. Serna, J. L. White, and S. L. Hem, *J. Pharm. Sci.*, **67**, 1081 (1978).

(8) J. M. Serrotosa and W. F. Bradley, *J. Phys. Chem.*, **62**, 1164 (1958).

(9) M. L. Jackson, "Soil Chemical Analysis Advanced Course," Department of Soils, University of Wisconsin, Madison, Wis., 1956, p. 35.

(10) J. R. Feldkamp and J. L. White, *J. Colloid Interface Sci.*, **69**, 97 (1979).

(11) H. van Olphen, "An Introduction to Clay Colloid Chemistry," Interscience, New York, N.Y., 1963, pp. 199–202.

(12) "Powder Diffraction File, Inorganic Volume," Joint Committee on Powder Diffraction Standards, Philadelphia, Pa., 1960.

(13) H. W. van der Marel and H. Bentelspacher, "Atlas of Infrared Spectroscopy of Clay Minerals and Their Admixtures," Elsevier, New York, N.Y., 1976.

(14) V. C. Farmer, "The Infrared Spectra of Minerals," Monograph 4, Mineralogical Society, London, England, 1974.

(15) J. L. White, *Soil Sci.*, **112**, 22 (1971).

(16) M. Barr, *J. Am. Pharm. Assoc.*, **NS4**, 4 (1964).

(17) "United States Dispensatory," 27th ed., Lippincott, Philadelphia, Pa., 1973, p. 182.

(18) J. F. Williams, B. C. Elsley, and D. J. Weintritt, *Clays Clay Miner.*, **2**, 141 (1953).

(19) J. R. Feldkamp, Ph.D. thesis, Purdue University, West Lafayette, Ind., 1978.

(20) W. T. Granquist and J. V. Kennedy, *Clays Clay Miner.*, **15**, 103 (1967).

(21) W. S. Stern, Ph.D. thesis, University of Michigan, Ann Arbor, Mich., 1971.

(22) G. Brown, "The X-Ray Identification and Clay Structures of Clay Minerals," 2nd ed., Jarrold and Sons, Norwich, England, 1961, p. 86.

(23) "Veegum: The Versatile Ingredient," Bulletin 15, R. T. Vanderbilt Co., Norwalk, Conn.

(24) C. S. Ross and S. B. Hendricks, U.S. Geological Survey, Paper 205B, 1945, p. 23.

(25) L. W. Zelazny and F. G. Calhoun, in "Minerals in Soil Environments," R. C. Dinauer, Ed., Soil Science Society of America, Madison, Wis., 1977, p. 445.

## ACKNOWLEDGMENTS

Supported in part by an American Foundation for Pharmaceutical Education Fellowship to J. E. Browne.

This report is Journal Paper 7953, Purdue University Agricultural Experiment Station, West Lafayette, IN 47907.